Tuberculosis 101 (2016) 174–190

Contents lists available at ScienceDirect

Tuberculosis

journal homepage: http://intl.elsevierhealth.com/journals/tube

MODEL SYSTEMS

Alternative BCG delivery strategies improve protection against *Mycobacterium tuberculosis* in non-human primates: Protection associated with mycobacterial antigen-specific CD4 effector memory T-cell populations

S. Sharpe [a, *], A. White [a], C. Sarfas [a], L. Sibley [a], F. Gleeson [b], A. McIntyre [b], R. Basaraba [c], S. Clark [a], G. Hall [a], E. Rayner [a], A. Williams [a], P.D. Marsh [a], M. Dennis [a]

[a] Public Health England, Porton Down, Wiltshire, SP4 0JG, UK
[b] Churchill Hospital, Headington, Oxford, UK
[c] Colorado State University, Fort Collins, CO, USA

ARTICLE INFO

Article history:
Received 31 May 2016
Accepted 11 September 2016

Keywords:
Tuberculosis
BCG
Biomarkers
Non-human primate
Aerosol challenge

ABSTRACT

Intradermal (ID) BCG injection provides incomplete protection against TB in humans and experimental models. Alternative BCG vaccination strategies may improve protection in model species, including rhesus macaques. This study compares the immunogenicity and efficacy of BCG administered by ID and intravenous (IV) injection, or as an intratracheal mucosal boost (ID + IT), against aerosol challenge with *Mycobacterium tuberculosis* Erdman strain. Disease pathology was significantly reduced, and survival improved, by each BCG vaccination strategy, relative to unvaccinated animals. However, IV induced protection surpassed that achieved by all other routes, providing an opportunity to explore protective immunological mechanisms using antigen-specific IFN-γ ELISpot and polychromatic flow cytometry assays. IFN-γ spot forming units and multifunctional CD4 T-cell frequencies increased significantly following each vaccination regimen and were greatest following IV immunisation. Vaccine-induced multifunctional CD4 T-cells producing IFN-γ and TNF-α were associated with reduced disease pathology following subsequent *M.tb* challenge; however, high frequencies of this population following *M.tb* infection correlated with increased pathology. Cytokine producing T-cells primarily occupied the CD4 transitional effector memory phenotype, implicating this population as central to the mycobacterial response, potentially contributing to the stringent control observed in IV vaccinated animals. This study demonstrates the protective efficacy of IV BCG vaccination in rhesus macaques, offering a valuable tool for the interrogation of immunological mechanisms and potential correlates of protection.

1. Introduction

Tuberculosis (TB) is a global health problem, with a third of the world's population estimated to be infected by *Mycobacterium tuberculosis* (M.tb); currently, there are 9 million new infections and 1.5 million deaths annually [1,2]. Bacille Calmette-Guréin (BCG), the only licenced TB vaccine protects children from developing severe TB [3]. However, the levels of protection conferred against pulmonary TB in adults are variable ranging from 0 to 80% depending on geographical location [4], and it is unsuitable for use in people whose immune system is compromised. Vaccination is widely accepted to be the most effective method for control of infectious disease, and improved vaccines against TB are desperately needed. A surrogate marker that could predict the potential efficacy of new vaccine candidates would accelerate the development process, but correlates of protection have yet to be identified. Without validated correlates, vaccine efficacy can only be determined though large scale clinical trials involving thousands of at-risk individuals in endemic countries [5]; such studies take a long time, are logistically complex and expensive. Preclinical animal models provide a critical component in the development process for new vaccines, as challenge studies can not only predict the effectiveness of vaccines in humans but they also provide the opportunity to identify and validate correlates of protection. Non-

* Corresponding author.
E-mail address: sally.sharpe@phe.gov.uk (S. Sharpe).

http://dx.doi.org/10.1016/j.tube.2016.09.004

human primates (NHP) provide the most relevant models of human tuberculosis because of their close similarity to humans [6–8], and, as in humans, intradermally (ID) delivered BCG affords macaques variable levels of protection against experimental challenge with *M. tb* (Langermans 2002, Verreck 2009, Sharpe 2010).

In the search to identify immune and or clinical biomarkers of disease and immune correlates of protection, a vaccine regimen inducing 100% protection would provide an invaluable tool. Studies published in the early 1970's revealed that BCG delivered intravenously (IV) gave superior protection to that afforded when it was delivered by other routes (intradermal (ID) subcutaneous (SC) or intramuscular (IM)) in rhesus macaques [9–12]. IV BCG therefore has the potential to improve upon the efficacy afforded by the conventionally used BCG vaccination and increase the opportunity to identify correlates of protection. BCG revaccination regimens using a primary and secondary ID vaccination have been shown to enhance protection against pulmonary *M. bovis* infection in cattle [13], provide improved early protection against *M.tb* in mice [14] and moderate improvements in protection against *M.tb* infection in people [15,16]; these improvements were dependant on geographical location of the study cohort. Murine studies suggest immunisation delivered directly to the respiratory mucosa may provide a more effective route of vaccination [17,18] and have indicated that intranasal delivery of a second BCG vaccination improved the outcome of *M. tb* challenge compared to a single ID BCG vaccination [19]. These studies taken together suggest that the efficacy afforded by multiple applications of BCG are improved by delivery of the second BCG vaccination to the lung.

There is no validated correlate of protection against *M.tb* infection but both a cell mediated T-helper 1 (Th1) response from CD4 T-cells [20] and an MHC-I restricted CD8 response [21] are known to be important for successful control of disease. In the absence of a true correlate, functional markers such as IFN-γ expression are measured to assess vaccine immunogenicity. There is evidence that the quality of the T-cell response is important to the induction of T-cell memory [22], and multifunctional CD4 cells expressing combinations of the cytokines IFN-γ, TNF-α and IL-2 are involved in the active phase of disease [23] and provide correlates of vaccine-induced protection [24–26], although not all reports support this latter role [27]. In addition to the induction of the specific effector T-cells (TEM) needed to execute inflammatory functions in the defence against *M. tb*, a successful TB vaccine will also need to induce persistent T-cell memory populations. Whilst TEM populations have been detected following systemic BCG vaccination [28], it has been hypothesised that the current BCG vaccination induces TEM populations capable of short term control of *M.tb* infection, but induces weakly the central memory T cell (TCM) populations required for long-term protection [29].

Previous macaque studies that have revealed the potential for route of delivery to enhance the efficacy afforded by BCG [9–12] were conducted at a time before the advent of modern immunological tools, which restricted the ability to interrogate the immune response and identify correlates of protection. This study sought to characterise the immunological profiles induced by BCG when delivered either intravenously or in an intradermal prime/mucosal boost regimen with the immunogenicity of ID-delivered vaccination, and by comparing the efficacy afforded by each vaccination delivery route against high dose *M.tb* aerosol challenge, elucidate potential correlates of protective immunity.

2. Materials and methods

2.1. Experimental animals

Twenty-four, three-year-old, male rhesus macaques of Indian genotype were obtained from an established UK breeding colony. Absence of previous exposure to mycobacterial antigens was confirmed by a tuberculin skin test and screening using an *ex-vivo* IFN-γ ELISPOT (MabTech, Nacka. Sweden) to measure responses to mycobacterial antigens: PPD (SSI, Copenhagen, Denmark), and pooled 15-mer peptides of ESAT6 and CFP10 (Peptide Protein Research LTD, Fareham, U.K.).

Animals were housed in compatible social groups, in accordance with the Home Office (UK) Code of Practice for the Housing and Care of Animals Used in Scientific Procedures (1989), and the National Committee for Refinement, Reduction and Replacement (NC3Rs), Guidelines on Primate Accommodation, Care and Use, August 2006 (NC3Rs, 2006). Animals were sedated by intramuscular (IM) injection of ketamine hydrochloride (Ketaset, 100 mg/ml, Fort Dodge Animal Health Ltd, Southampton, UK; 10 mg/kg) for procedures requiring removal from their housing. None of the animals had been used previously for experimental procedures and each socially compatible group was randomly assigned to a particular study treatment. All animal procedures and study design were approved by the Public Health England, Porton Down Ethical Review Committee, and authorized under an appropriate UK Home Office project license.

2.2. Vaccination

A plan of the vaccination strategy and timing of the aerosol challenge is shown in Fig. 1. Twelve animals (groups A and B) were immunised ID in the upper left arm with 100 μl BCG vaccine, Danish strain 1331 (SSI, Copenhagen, Denmark). Six animals (group C) were immunised IV with 1000 μl BCG vaccine into the femoral vein of the left leg. Twelve weeks after primary ID vaccination, 6 animals (group B) received a second vaccination with 1000 μl BCG vaccine delivered using an endotracheal catheter gauge 8 FG inserted into the lung to a depth of 15 cm, with the catheter flushed through using 0.5 ml sterile PBS. BCG vaccine was prepared for intradermal or intravenous administration according to manufacturer's instructions for preparation of vaccine for administration to human adults. This involved by addition of 1 ml Sautons diluent to a vial of vaccine, to give a suspension of BCG at an estimated concentration of 2×10^6 to 8×10^6 CFU/ml. Seven vials of reconstituted vaccine were combined to provide the preparation for IV inoculation. For delivery to the lung, four vaccine vials were each reconstituted with 1 ml of sterile PBS and combined together immediately prior to administration to give an estimated concentration of 2×10^7 to 8×10^7 CFU/ml. Vaccinations were administered within 1 h of vaccine reconstitution. The viability of the BCG vaccine was confirmed to be within the expected range for the batch on each occasion. The intradermal vaccination sites were monitored and assessed for local reactions after vaccination with BCG.

2.3. M. tuberculosis challenge strain

The Erdman K01 stock (HPA-Sept 2011) used for challenge was prepared from stocks of the *M. tuberculosis* Erdman strain K 01 (BEI Resources). A stock suspension was initially prepared from a 5 ml bacterial starter culture originally generated from colonies grown on Middlebrook 7H11 supplemented with oleic acid, albumin, dextrose and catalase (OADC) selective agar (BioMerieux, UK). A liquid batch culture was then grown to logarithmic growth phase in 7H9 medium (Sigma-Aldrich, UK) supplemented with 0.05% (v/v) Tween 80 (Sigma-Aldrich, UK). Aliquots were stored at −80 °C. The titre of the stock suspension was determined from thawed aliquots by enumeration of colony forming units cultured onto Middlebrook 7H11 OADC selective agar.

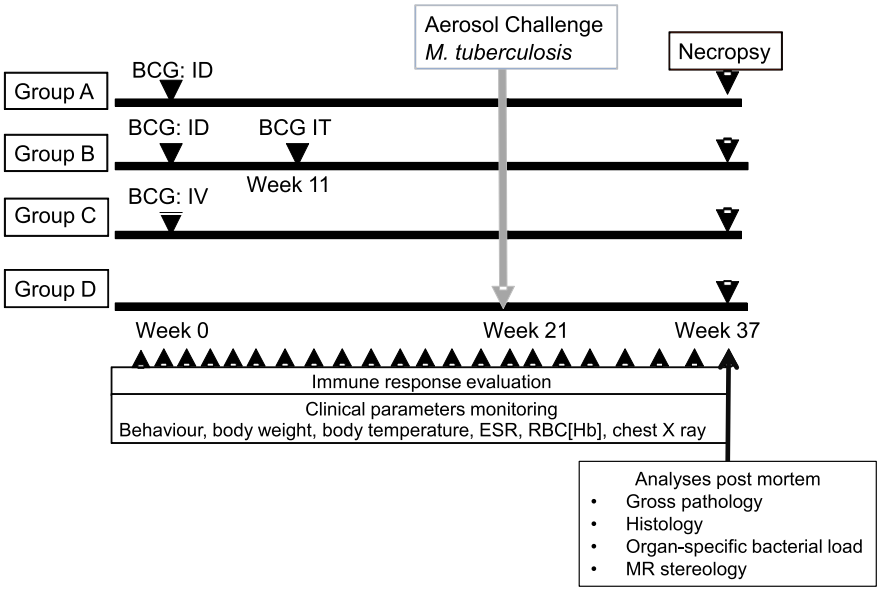

Fig. 1. Experimental study design.

2.4. Aerosol exposure

Twenty one weeks after primary vaccination of animals in groups A, B and C with BCG, the immunised animals, together with six unvaccinated animals (Group D), were challenged by exposure to aerosols of *M. tb* (Fig. 1). as previously described [30–32]. Monodispersed bacteria in particles were generated using a 3-jet Collison nebuliser (BGI) and, in conjunction with a modified Henderson apparatus [33], delivered to the nares of each sedated primate via a modified veterinary anaesthesia mask. Challenge was performed on sedated animals placed within a 'head-out', plethysmography chamber (Buxco, Wilmington, North Carolina, USA) to enable the aerosol to be delivered simultaneously with the measurement of respired volume. The aerosol delivery process was designed to result in the deposition of a target dose of 100 CFU in the lungs. The number of bacilli deposited and retained in the lungs of macaques cannot be measured directly and quantification of the dose must be calculated from the concentration of viable organisms in the aerosol (C_{aero}) and the volume of aerosol inhaled by the animal. This 'presented dose' (PD) is the number of organisms that the animals inhale. C_{aero} is either measured directly using air sampling within the system or may be calculated using the concentration of organisms in the nebulizer (C_{neb}) and a 'spray factor' that is a constant derived from data generated for the specific organism with identical aerosol exposure parameters. The calculations to derive the PD and the retained dose (the number of organisms assumed to be retained in the lung) have been described previously for high/medium aerosol doses [30,31]. The assumed retained dose was calculated from the PD by applying a retention factor. Retention factors for rhesus macaques are described by Harper and Moreton [34]. Challenge was conducted such that one animal from each group was exposed in sequence (in the group order D, A, B, C) with the cycle repeated until all animals were exposed.

2.5. Clinical procedures

Animals were monitored daily for behavioural abnormalities including depression, withdrawal from the group, aggression, and clinical changes in feeding patterns, respiration rate and coughing. On each occasion that required blood sample collection, aerosol challenge or euthanasia, animals were weighed, rectal temperature measured and examined for gross abnormalities. Red blood cell (RBC) haemoglobin levels were measured using a HaemaCue haemoglobinometer (Haemacue Ltd, Dronfield, UK) to identify the presence of anaemia, and erythrocyte sedimentation rates (ESR) were measured using the Sediplast system (Guest Medical, Edenbridge, UK) to detect and monitor inflammation induced by infection with *M. tb*.

The time of necropsy, if prior to the end of the planned study period, was determined by experienced primatology staff and based on a combination of the following adverse indicators: depression or withdrawn behaviour, abnormal respiration (dyspnoea), loss of 20% of peak post-challenge weight, ESR levels elevated above normal (>20 mm), haemoglobin level below normal limits (<100 g/dL), increased temperature (>41 °C) and severely abnormal thoracic radiograph.

2.6. Immune response analysis: Interferon-gamma (IFN-γ) ELISpot

Peripheral blood mononuclear cells were isolated from heparin anti-coagulated blood using standard methods. An IFN-γ ELISpot assay was used to estimate the number of, and IFN-γ production capacity of, mycobacteria-specific T cells in PBMCs using a human/simian IFN-γ kit (MabTech, Nacka. Sweden), as described previously [31]. In brief, PBMCs were cultured with 10 μg/ml PPD (SSI, Copenhagen, Denmark), or without antigen, in triplicate, and incubated for 18 h. Phorbol 12-myristate (Sigma-Aldrich Dorset, UK) (100 ng/ml) and ionomycin (CN Biosciences, Nottingham, UK) (1 μg/ml) were used as a positive control. After culture, spots were developed according to the manufacturer's instructions. Determinations from triplicate tests were averaged. Data were analysed by subtracting the mean number of spots in the cells for medium-only control wells from the mean counts of spots in wells with cells and antigen or peptide pools.

2.7. Intracellular cytokine staining and memory T-cell analysis

2.7.1. Polyfunctional intracellular cytokine staining and antigen-specific memory T-cell assay

Intracellular cytokine staining (ICS) was performed using

1×10^6 PBMC in medium (R10) consisting of RPMI 1640 supplemented with L-glutamine (2 mM), penicillin (50 U/ml) streptomycin (50 μg/ml) (all from Sigma Aldrich, Gillingham, UK) and 10% heat-inactivated foetal bovine serum (Labtech Ltd, Uckfield, UK). These cells were stimulated with a 10 μg/ml solution of CD28 and CD49d co-stimulatory antibodies (both from BD Biosciences, Oxford, UK) and either 10 μg/ml PPD (SSI, Copenhagen, Denmark), 5 μg/ml SEB (Sigma Aldrich, Gillingham, UK), or R10 medium alone as negative control, for a total of 6 h at 37 °C, in a 5% CO_2 supplemented incubator. Following the initial 2 h of incubation, the protein transport inhibitor Brefeldin-A (Sigma Aldrich, Gillingham, UK) was added to the incubation mixture at a final concentration of 10 μg/ml. Following incubation, cells were washed with FACS buffer consisting of PBS +1% FCS and incubated for 30 min at room temperature with optimal dilutions of the amine-reactive Live/Dead Fixable Red viability cell stain (Life Technologies, Renfrew, UK) and the antibodies CD4 APC-H7, CD8 PerCP-Cy5.5, CD95 Pe-Cy7 (all from BD Biosciences, Oxford, UK), CD28 BV-421 (Biolegend, London, UK), CCR7-PE (eBioscience, Hatfield, UK), CD14-ECD and CD20-ECD (both from Beckman Coutler, High Wycombe, UK). Following surface marker staining, the cells were washed and then permeabilised by incubation at room temperature for 15 min with Fix/Perm reagent (BD Biosciences, Oxford, United Kingdom). Further cell washes were applied using Permwash buffer (BD Biosciences, Oxford, United Kingdom), before staining for intracellular antigens by incubation at room temperature for 30 min with the antibodies CD3-AF700, IFN-γ-FITC, TNF-α-BUV395 (all from BD Biosciences, Oxford, United Kingdom), and IL-2-APC (Miltenyi Biotech Ltd, Bisley, UK). BD Compbeads (BD Biosciences, Oxford, UK) were labelled with the above fluorochromes for use as compensation controls. Following antibody labelling, cells and beads were washed by centrifugation and fixed in 4% paraformaldehyde solution (Sigma Aldrich, Gillingham, UK) prior to flow cytometric acquisition.

2.7.2. Flow cytometric acquisition and analysis

Cells were analysed using a five laser LSRII Fortessa instrument (BD Biosciences, Oxford, UK) and data were analysed using FlowJo (version 9.7.6, Treestar, Ashland, US). Cytokine-producing T-cells were identified using a forward scatter-height (FSC-H) versus side scatter-area (SSC-A) dot plot to identify the lymphocyte population, to which appropriate gating strategies were applied to exclude doublet events, non-viable cells, monocytes ($CD14^+$) and B cells ($CD20^+$). For ICS analysis, sequential gating through $CD3^+$, followed by $CD4^+$ or $CD8^+$ gates were used before individual cytokine gates to identify IFN-γ, IL-2 and TNF-α producing populations. Polyfunctional cells were identified using Boolean gating combinations of individual cytokine-producing CD4 or CD8 T-cells. Antigen-specific T-cell memory profiles were identified by applying a summed CD4 or CD8 cytokine Boolean combination, followed by gating for CD95 surface staining. Differentiation of effector to central memory T-cell populations was established by CD28 and CCR7 expression (Figs. 5 and 6). The software package PESTLE (version 1.7) was used for background subtraction to obtain antigen-specific polyfunctional ICS and memory T-cell cytokine responses, and SPICE (version 5.35) was used to generate graphical representations of flow cytometry data (Mario Roederer, Vaccine Research Centre, NIAID, NIH).

2.8. Necropsy

Animals were anaesthetised and clinical data collected. Blood samples were taken prior to euthanasia by intra-cardiac injection of a lethal dose of anaesthetic (Dolelethal, Vétoquinol UK Ltd, 140 mg/kg). A post-mortem examination was performed immediately and gross pathological changes were scored using an established system based on the number and extent of lesions present in the lungs, spleen, liver, kidney and lymph nodes, as described previously [Sharpe 2010]. Samples of spleen, liver, kidneys and tracheobronchial, inguinal and axillary lymph nodes were removed and sampled for quantitative bacteriology. The lungs, including the heart and lung-associated lymph nodes, were removed intact. The lymph nodes were measured and examined for lesions. The complete lung set was fixed by intra-tracheal infusion with 10% neutral buffered formalin (NBF) using a syringe and 13CH Nelaton catheter (J.A.K. Marketing, York, UK). The catheter tip was inserted into each bronchus in turn via the trachea; the lungs were infused until they were expanded to a size considered to be normal inspiratory dimensions, and the trachea ligated to retain the fluid. The infused lung was immersed in 10% NBF. In addition, samples of kidneys, liver, spleen, and sub-clavicular, hepatic inguinal and axillary lymph nodes were fixed in 10% NBF.

2.9. Lung imaging

Thoracic radiographs (SP VET 3.2, Xograph Ltd) were acquired using mammography film (Xograph Imaging Systems Ltd, Tetbury, UK) before and every 2 weeks after exposure to *M. tb*. Evaluation of disease was performed by an experienced consultant thoracic radiologist blinded to the animal group and clinical status using a pre-determined scoring system based on the amount and distribution of infiltrate. The lung was divided into four zones (left and right sides divided at the anterior aspect of the fifth rib) and the disease burden scored in each area according to the system 0 = normal; 1 =<10% abnormal; 2 => 10% < 50% abnormal; 3 => 50% < 75% abnormal; 4 => 75% abnormal. The scores for each zone were summed to provide the total radiographic score where the maximum score was 16.

2.10. Magnetic resonance imaging

The *ex-vivo* expanded, fixed lungs were set in 2% agarose (Sigma-Aldrich, UK) and images were taken using a 3.0 T 750 MRI Scanner (General Electric Healthcare, Milwaukee, WI, USA) as described previously [31]. This enabled evaluation of the pulmonary disease burden at the end of the study period. Lung lesions were identified in MR images from their signal intensity and nodular morphology relative to normal lung parenchyma.

2.11. Lesion analysis/quantification (Stereology)

Lung lesions were identified on MR images based on their signal intensity and nodular morphology relative to more normal lung parenchyma. The total lung and lesion volume relative to the fixed tissue was determined using the Cavalieri method applied to MRI image stacks, and then expressed as a ratio to provide a measure of disease burden in each animal, as previously described [31,32]. Analyses of lesion volume on magnetic resonance (MR) images were performed with the investigators reading the images blind to treatment groups.

2.12. Pathology studies

The fixed lungs were removed from the agar, sliced serially and lesions counted as described previously [35]. Each lung lobe was evaluated separately and discrete lesions were counted in the parenchyma. Where lesions had coalesced, these were measured and recorded. Lung-associated lymph nodes, particularly around the tracheal bifurcation, were dissected and weighed. The remaining tissues were examined during trimming.

2.13. Histopathological examination

Representative samples from each lung lobe and other organs, were processed to paraffin wax, sectioned at 3–5 μm and stained with haematoxylin and eosin (HE). For each lung lobe, tissue slices containing obvious lesions were chosen for histological examination. Where gross lesions were not visible, a sample was taken from a predefined anatomical location from each lobe to establish consistency between animals. Sections of lung associated lymph nodes. The nature and severity of the microscopic lesions was evaluated subjectively by a pathologist who was blinded to prevent bias. In the lung, each lobe section was assigned a consolidation score as follows: no abnormality = 0; very small, very few lesions, <10% consolidation = 1; few or small lesions, 10–20% consolidation = 2; medium sized lesions, 20–33% consolidation = 3; moderately sized lesions, 33–50% consolidation = 4; large lesions, moderately extensive pneumonia, 50–80% consolidation = 5; extensive pneumonia >80% consolidation = 6. A total score for each lung, and mean consolidation score per lobe, was calculated for each group. In non-pulmonary tissue, the occurrence of tuberculosis was scored as present or absent.

2.14. Bacteriology

The spleen, kidneys, liver and tracheobronchial lymph nodes were sampled for the presence of viable *M.tb* post-mortem [32]. Weighed tissue samples were homogenized in 2 ml of sterile water, and either serially diluted in sterile water prior to being plated or plated directly onto Middlebrook 7H11 OADC selective agar. Plates were incubated for 3 weeks at 37 °C and resultant colonies were confirmed as *M.tb* and counted.

2.15. Statistical analyses

Comparison of *ex-vivo* ELISpot assay responses was completed using the area under the curve (AUC) of each animal's response calculated using Sigmaplot version 10 (Systat Software Inc, Hounslow, UK). AUC values were compared between test groups using the non-parametric Mann-Whitney *U* test, Minitab version 15 (Minitab Ltd, Coventry, UK). To compare T-cell functional and memory profiles measured by polyfunctional flow cytometry, T-cell subset frequencies measured in each vaccination group were compared using a Wilcoxon-rank test at each analysis time-point (SPICE v 5.35). Similarly, vaccine-induced changes in T-cell functional profiles within each vaccination group were assessed by comparing frequencies at each analysis time-point with mean baseline values. Negative values in antigen-specific ICS data generated by background subtraction were replaced by a minimum threshold value [36].

Differences in the pathology scores, pulmonary disease measures and clinical measures of disease burden at the end of study were compared between test groups using the non-parametric Mann-Whitney *U* test, Minitab version 15 (Minitab Ltd, Coventry, UK). Differences in the survival rates of animals in each test group were compared with a log rank test using Minitab version 15 and Gehan-Breslow-Wilcoxon test in Graphpad Prism, version 5.01 (GraphPad Software Inc, La Jolla, California, USA).

The Spearman correlation test was used to determine the level of correlation between study parameters using GraphPad Prism, version 5.01 (GraphPad Software Inc, La Jolla, California, USA).

3. Results

3.1. Safety of BCG delivery by alternative routes

All animals in the study showed the weight gain profiles expected in normal healthy animals during the period prior to challenge. Temperature, erythrocyte sedimentation rate (ESR) and red cell haemoglobin levels all remained within the normal range during the post-vaccination and pre-challenge phase of the study. Mild induration and erythema occurred at the site of BCG immunisation in animals that received an intradermal vaccination with BCG. Reactions appeared four weeks after BCG vaccination and were completely resolved in animals by 16 weeks after immunisation. Both intravenous and intra-tracheal delivery of BCG were well tolerated and neither led to perturbations beyond normal ranges in the clinical parameters measured.

3.2. M. tuberculosis exposure and disease progression post-challenge

The macaques were challenged with a median estimated retained dose of 94 cfu (range 74–174) (Table 1) and the doses were consistent across all the study groups. In the period after aerosol challenge with *M. tb*, a proportion of animals in all four study groups showed changes in behaviour and clinical parameters consistent with progression of tuberculosis-induced disease and were euthanized ahead of the planned end of the study. These animals included five of the six naïve control group D (S23, S33, S36, S40, S51), three of six ID BCG-vaccinated animals in group A (S43, S6, S17), two of six ID + IT BCG vaccinated animals in group B (S42, S12) and one of six IV BCG vaccinated animals in group C (S35), and all exhibited progressive weight loss, elevated ESR levels, erythrocyte haemoglobin concentrations below the normal range, tachypnoea and or dyspnoea and cough (red symbols, Fig. 2E–H). None of the surviving animals in any vaccination group showed adverse behavioural or pre-mortem clinical indicators at the time of termination 17–20 weeks after challenge (Fig. 2E–H).

The length of time that the animals in each group controlled disease before levels progressed to reach clinical end-points (Fig. 3) was compared using two statistical approaches: the Log Rank Test and the Gehan-Breslow-Wilcoxon Test. Comparison of survival times between each of the vaccination groups A, B and C and the unvaccinated control group D revealed BCG vaccination improved the control of TB-induced disease in the first 17 weeks following aerosol challenge. The difference in survival time reached statistical significance using the Log rank test only when BCG was given intravenously (P = 0.017), although the Gehan-Breslow-Wilcoxon test suggested the differences to be significant for all three BCG vaccination regimens (IV: $p = 0.02$; ID: $p = 0.05$; ID + IT: $p = 0.05$). Differences in survival time between vaccination groups were not revealed by either test, between the group vaccinated with ID BCG alone and the IV BCG vaccinated group.

3.3. Measures of tuberculosis-induced disease burden

At the end of the study, the level of tuberculosis-induced disease burden was determined using a range of approaches that have been used previously for the evaluation of TB vaccine efficacy in a rhesus macaque aerosol challenge model [31] (Fig. 2). TB-induced disease burden was higher in animals that met humane endpoint criteria during the study than in those that controlled disease progression to the end of the study. The gross pathology score determined at necropsy, based on the number and size of lesions, revealed the level of disease in all BCG vaccinated groups to be significantly lower than in the unvaccinated group in all groups (BCG IV: $p = 0.01$, BCG ID: $p = 0.05$ and BCG ID/IT: $p = 0.05$). Intravenous vaccination with BCG also afforded a significant improvement over ID BCG vaccination ($p = 0.04$) (Fig. 2D).

Table 1
Aerosol challenge doses of *M. tuberculosis* delivered to rhesus macaques.

Group	Vaccine and route	Animal Identification number	Presented Dose (cfu)	Estimated Retained Dose (cfu)
Group A	BCG ID	S6	571	82
		S14	535	76
		S17	666	95
		S22	632	90
		S26	1215	174
		S43	627	90
Group B	BCG ID + IT	S12	647	92
		S24	714	102
		S42	773	111
		S45	525	75
		S58	535	76
		S63	802	115
Group C	BCG IV	S4	688	98
		S7	812	116
		S19	744	106
		S20	447	64
		S35	1016	145
		S61	802	115
Group D	No vaccine	S23	515	74
		S33	525	79
		S36	1176	168
		S40	972	139
		S51	622	89
		S50	539	77
		Study median	657	94

Route of delivery: ID: intradermal; IV: intravenous; IT: intratracheal.

3.4. Pulmonary disease burden

The pathology and imaging measures used to assess pulmonary disease burden showed similar trends in outcome (Table 2). The number of pulmonary lesions determined by serial sectioning and manual counting of both discrete and coalesced lesions (Fig. 2B), and the lung pathology scores (Fig. 2C), were significantly less in the BCG IV and BCG ID/IT groups than in the unvaccinated group. Lung lesion counts also revealed IV vaccination with BCG afforded a significant improvement over ID vaccination with BCG. Thoracic radiographic scores (Fig. 2E), pulmonary disease burden quantified using stereology on MR images to determine the ratio between total lesion volume and lung volume (Fig. 2 A), and terminal measures of clinical parameters (Fig. 2F, G, H) revealed similar generally non-significant trends for the highest disease burden to occur in the unvaccinated group, lower levels of disease in the BCG ID and BCG ID/IT vaccinated groups, and the lowest level of disease in the BCG IV group. There was a trend for the erythrocyte sedimentation rate (ESR) to be lower in the BCG IV vaccinated group than in the unvaccinated group, and red blood cell haemoglobin concentrations were greater in the BCG ID/IT group than in the unvaccinated group.

Microscopic, lung consolidation scores were highest in the unvaccinated group (score = 148) compared to the vaccinated groups (ID score = 104; ID/IT score = 99; IV score = 80); furthermore, discrete granulomas in this group lacked a fibrous capsule. Lesions in animals that received an intradermal vaccination with BCG were less severe than those in the unvaccinated animals, but less well organised than those in the BCG IV or BCG ID/IT vaccinated animals, where granulomas had a caseated, occasionally calcified centre, and evidence of peripheral fibrosis.

3.5. Extra-pulmonary disease burden

Evidence of dissemination to the hilar lymph nodes, liver, kidneys and spleen was evaluated by microscopic examination and by culture of tissue samples for the presence of viable *M. tb* (Table 3). Microscopic lesions were found more frequently in non-pulmonary tissues from unvaccinated animals and BCG ID vaccinated animals than in tissues from BCG ID/IT and BCG IV vaccinated animals (Table 3). Similarly, *M. tb* was isolated from a reduced number of the tissues collected from the BCG IV, or ID/IT vaccinated animals compared to the tissues from the BCG ID, or unvaccinated groups (Table 3). Where bacteria were isolated, the bacterial burden in tissues was at a similar level in all study groups.

Taken together the results of microscopic examination and bacterial culture show a lower level of disseminated disease in the BCG IV vaccinated group as evidence of TB was only detected in a single animal (S35) in the spleen, liver and kidneys, in the liver and kidneys of a second animal (S20), and the kidneys of a third animal (S4). In contrast, evidence of TB was found in the spleen, liver and kidneys of all the unvaccinated animals, and the majority of the BCG ID vaccinated animals (liver, six of six, spleen and kidneys five of six). Dissemination frequency to the liver in the BCG ID/IT group was equivalent to the BCG ID and unvaccinated groups; however, there was a trend for reduced spread to the spleen (two of six) and kidneys (three of six).

3.6. Immune response correlates

3.6.1. IFN-γ response to vaccination/aerosol challenge with *M. tuberculosis*

The mycobacterium-specific IFN-γ response induced by vaccination and challenge was measured using an *ex-vivo* ELISpot assay applied at two weekly intervals through the study (Fig. 4) and revealed differences in the response profiles of PPD-specific IFNγ secreting cells in BCG vaccinated and unvaccinated animals. The response to BCG vaccination reached a peak six weeks after intravenous (group C Fig. 4C), or intradermal administration (group A, Fig. 4 A). The response profile in BCG ID/IT immunised animals (group B) showed a second peak at week 12, one week after intratracheal delivery of the second dose of BCG (Fig. 4B). During the same period, responses remained uniformly low in the unvaccinated animals (group D, Fig. 4D). The frequency of PPD-specific IFN-γ secreting cells was significantly higher in BCG vaccinated groups (Group A, ID versus Group D: $p = 0.005$; Group ID/IT versus Group

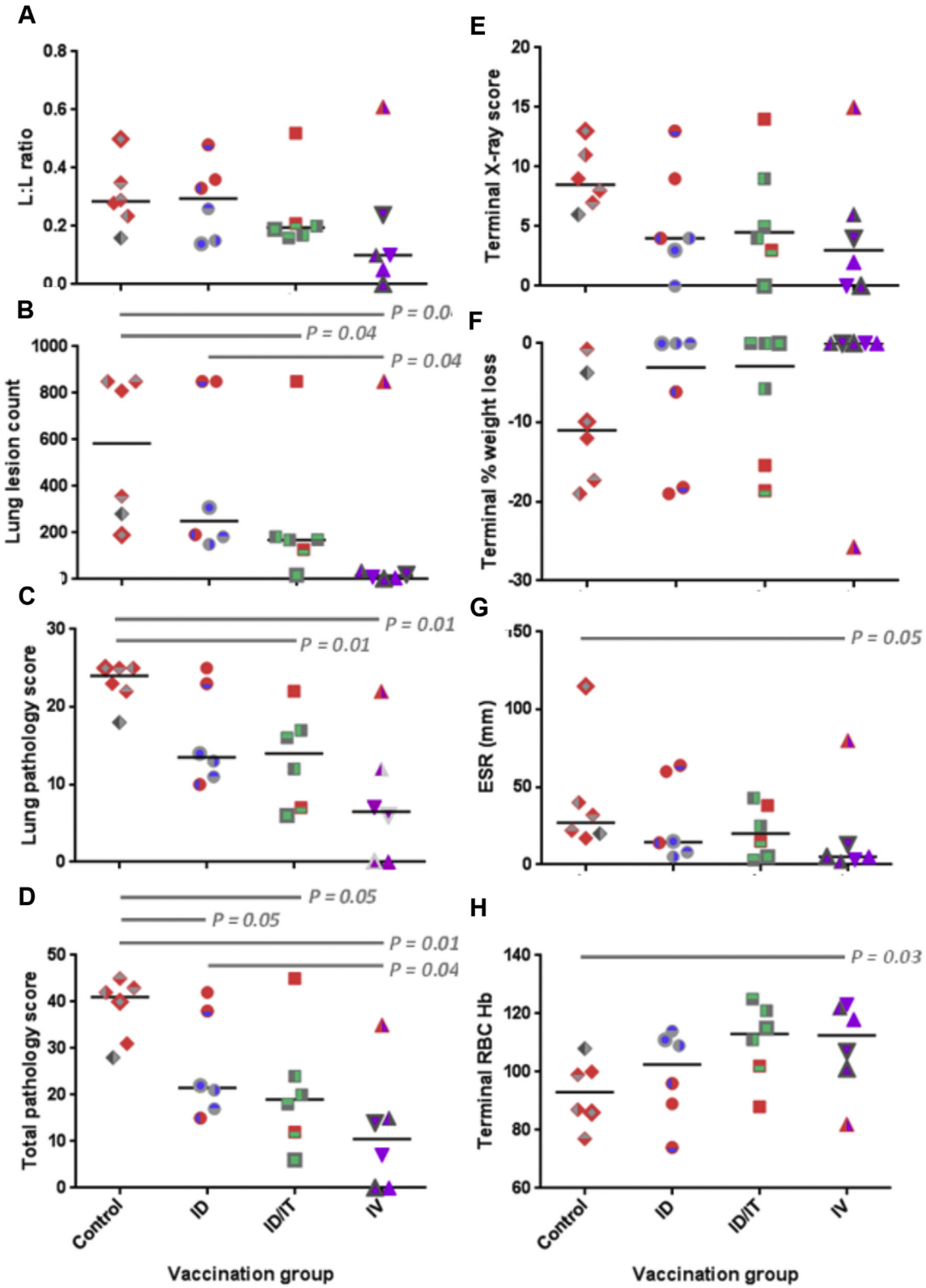

Fig. 2. Measures of tuberculosis-induced pulmonary and clinical disease burden. Panel A: the lung to lesion volume ratio determined using MR stereology; Panel B: number of lesions in the lung enumerated by serial sectioning and manual counting; Panel C: the score attributed to the pulmonary component as part of the total pathology; Panel D: the total pathology score determined using a qualitative scoring system; Panel E: score attributed to the chest radiogram on the day of euthanasia; Panel F: % weight loss from peak post-challenge weight on the day of euthanasia; Panel G: Erythrocyte sedimentation rate (ESR) on the day of euthanasia; Panel H: bacterial load in the lung. Red shading indicates animals in which disease reached endpoint criteria. P values are shown and * denotes significant difference in outcome between groups using the non-parametric Mann-Whitney *U* test, $p \leq 0.05$.

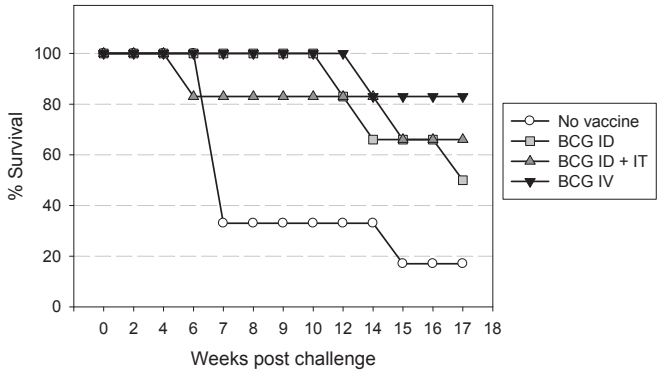

Fig. 3. Kaplan Meier plot of survival of vaccinated and unvaccinated NHPs after challenge with *M. tuberculosis*.

Table 2
Statistical analysis of the differences between test groups using different vaccine efficacy readouts.

Measure	P Value*				
	Test group compared to No vaccine			Test group compared to BCG ID	
	BCG ID	BCG ID/IT	BCG IV	BCG ID/IT	BCG IV
Lesion: Lung volume	0.81	0.26	0.13	0.81	0.13
Lung lesion Count	0.46	**0.04**	**0.04**	0.10	**0.04**
Pathology Score	**0.05**	**0.05**	**0.01**	0.58	**0.04**
Lung score	0.08	**0.01**	**0.01**	0.58	0.07
Thoracic radiograph	0.17	0.20	0.08	0.87	0.63
% weight loss	0.41	0.29	0.06	0.86	0.45
RBC [Hb]	0.38	0.03	0.09	0.81	0.17
ESR	0.23	0.38	**0.05**	0.20	0.30

• Mann Whitney test. Route of delivery: ID: intradermal; IV: intravenous; IT: intratracheal.
Bold text indicates values less than or equal to 0.05. P ≤ 0.05.

D: $p = 0.005$; Group C IV versus Group D: $p = 0.005$) than in unvaccinated animals in the period between vaccination and challenge. The group that received BCG by the intravenous route made the largest PPD-specific response during the 20 week period after vaccination, and statistical analysis using AUC and Mann Whitney tests confirmed the response to be significantly greater than the responses induced by BCG following either a single intradermal vaccination ($p = 0.005$) or an intradermal prime - intratracheal boost regimen ($p = 0.0202$). The PPD-specific IFN-γ secreting cell profile induced by the BCG ID prime/IT boost regimen, although increased, was not significantly different to the profile induced by a single intradermal BCG vaccination ($p = 0.093$) over the 20 week period. However, between weeks 12 and 20, the second BCG vaccination in the regimen boosted the response to a level comparable to that detected following BCG IV vaccination ($p = 0.689$), and greater than that in the BCG ID vaccination group ($p = 0.031$). Responses measured 20 weeks after vaccination just prior to challenge were significantly greater in both the BCG IV group ($p = 0.005$) and the BCG ID prime/IT boost group ($p = 0.03$) than in the unvaccinated control group, in contrast to response in the BCG ID group ($p = 0.11$).

After aerosol challenge with *M. tb,* the PPD-specific IFN-γ responses induced in the BCG vaccinated groups (A, B, C) were lower than those induced in the unvaccinated group (D) and lowest in group C which received BCG by intravenous injection. Statistical comparison of responses between test groups was only valid in the early phase after infection while all animals remained in the study. Analysis of the responses during the first four weeks after infection verified the PPD-specific IFN-γ response to be significantly lower in BCG vaccinated groups (Group A, ID versus Group D no vaccine: $p = 0.031$; Group B ID/IT versus Group D, no vaccine: $p = 0.005$; Group C IV versus Group D, no vaccine: $p = 0.005$) than in the unvaccinated animals. The responses measured in the groups that received BCG, either intravenously (group C) or in an ID/IT prime boost regimen (group B), were equivalent ($p = 0.34$) and both were significantly lower than the response measured in the group that received BCG by intradermal injection ($p = 0.005$).

The Spearman's Rank correlation test was applied to evaluate potential relationships between the frequency of PPD-specific IFN γ secreting cells induced by vaccination, or challenge and the TB-induced disease burden evaluated at termination using a range of measures, including gross pathology score, pulmonary lesion counts, lesion to lung volume ratio and changes in clinical parameters. Significant relationships between measures were not identified within individual test groups.

When results from all animals in the study were combined and tested, a higher frequency of IFNγ secreting cells (AUC) during the 20 week period after vaccination showed a statistically significant correlation with lower disease burden after challenge (total pathology score $p = 0.004$, lung score, $p = 0.002$, pulmonary lesion count, $p = 0.005$, % weight loss, $p = 0.012$, terminal ESR $p = 0.04$, terminal red blood cell haemoglobin concentration, p = 0.03). Similarly, a high frequency of IFNγ secreting cells after challenge significantly correlated with decreased survival time and higher levels of disease burden measured.

3.6.2. Polyfunctional CD4 and CD8 T-cell profiles

Frequencies of CD4 and CD8 T-cells producing combinations of the cytokines IFN-γ, IL-2 and TNF-α in response to antigenic stimulation with tuberculin PPD were measured in PBMC samples collected at selected time points throughout the study. Antigen specific CD4 T-cells were found to primarily occupy three distinct functional profiles, which were producing all three cytokines simultaneously (polyfunctional T-cells), IFN-γ and TNF-α in unison, or TNF-α alone (Fig. 5a). Frequencies of multiple cytokine producing CD4 T-cell populations increased significantly relative to pre-vaccination levels following both ID and IV vaccination in all immunisation groups ($P \leq 0.04$). Polyfunctional populations were apparent from six weeks following IV BCG vaccination but remained undetected in other vaccination groups until week 10 (Fig. 5a). There was a trend for higher frequencies of multifunctional CD4 T-cells to be detected during the vaccination phase (up to week 20) following IV vaccination, and this response persisted throughout the post-vaccination period. Comparisons between the groups revealed that these elevated frequencies only reached statistical significance at study week 12, relative to the ID BCG vaccination group ($p = 0.025$). An increased frequency of IFN-γ and TNF-α dual cytokine secreting cells, suggestive of a boosting response, was apparent in the ID + IT vaccination group one week after intratracheal BCG inoculation. However, this was not found to be significantly different from frequencies of the equivalent population measured in either the ID or IV vaccinated animals ($p = 0.055$ and 0.75, respectively), although the difference between ID and ID + IT vaccinated groups approached statistical significance.

M.tb aerosol challenge induced an anamnestic CD4 T-cell response in the ID and ID + IT vaccinated animals, as shown by increased frequencies of polyfunctional T-cells and those producing IFN-γ and TNF-α simultaneously four weeks following exposure. However, frequencies remained low in IV vaccinated animals relative to other vaccination groups and unvaccinated controls, and were comparable to levels detected during the vaccination phase of

Table 3
Evidence of extra-pulmonary TB-induced disease from microscopic examination and bacterial culture.

Group	Vaccine	ID	Evidence of TB															
			Hilar LN				Spleen				Liver				Kidney			
			Individual		Group (N/6)		Individual		Group (N/6)		Individual		Group(N/6)		Individual		Group(N/6)	
			M	BC	M	BC	M	BC	M	BC	M	BC	M	BC	M	BC	M	BC
A	BCG	S6	+	+			+	+			+	+			+	+		
	ID	S14	+	+			+	+			+	+			+	−		
		S17	+	+	6	6	+	+	4	5	+	+	5	4	+	+	5	3
		S22	+	+			−	−			+	−			+	−		
		S26	+	+			+	+			+	−			+	−		
		S43	+	+			+	+			−	+			−	+		
B	BCG	S12	+	+			−	+			+	+			+	+		
	ID + IT	S24	+	−			−	−			+	−			−	−		
		S42	+	+	6	5	−	−	0	2	+	+	5	3	+	−	3	2
		S45	+	+			−	−			+	−			−	−		
		S58	+	+			−	−			+	+			+	+		
		S63	+	+			−	+			−	−			−	−		
C	BCG	S4	+	−			−	−			−	−			+	−		
	IV	S7	−	−			−	−			−	−			−	−		
		S19	−	+	4	3	−	−	1	1	−	−	2	1	−	−	3	1
		S20	+	−			−	−			+	−			+	−		
		S35	+	+			+	+			+	+			+	+		
		S61	+	+			−	−			−	−			−	−		
D	No Vaccine	S23	+	+			−	+			+	+			+	+		
		S33	+	+			+	+			+	+			+	+		
		S36	+	+	6	5	+	+	5	6	+	+	6	6	+	+	6	6
		S40	+	+			+	+			+	+			+	+		
		S51	+	+			+	+			+	+			+	+		
		S50	+	−			+	+			+	+			+	+		

ID: Identification number; LN: lymph node; M: microscopic examination; BC: bacterial culture; −: feature not present; +: feature present; N/6 where N is the number of animals in which evidence of TB infection was determine in the tissue by either bacterial culture or microscopic examination. Route of delivery: ID: intradermal; IV: intravenous; IT: intratracheal.

the study. A population of TNF-α only secreting CD4 T-cells were detected in the IV and ID + IT vaccination groups following *M.tb* aerosol challenge, but not in animals receiving ID BCG or no vaccination. *M.tb* specific immune responses in the unvaccinated control group did not exceed baseline levels until four weeks after *M.tb* aerosol challenge.

A Spearman's rank correlation analysis applied to determine the dependence between cytokine producing CD4 T-cell frequency and disease outcome indices measured at necropsy revealed a weak, but significant, negative correlation between the frequency of CD4 T-cells simultaneously producing IFN-γ and TNF-α measured in vaccinated animals at study week 6, and reduced lung and total pathology score ($p = 0.005$ and $p = 0.018$, respectively) (Fig. 6a and b). Furthermore, the inverse relationship was observed when this analysis was repeated using CD4 T-cell frequencies measured four weeks following *M.tb* challenge, with greater IFN-γ and TNF-α producing multifunctional CD4 T-cell frequencies correlating with increased lung and total pathology ($p = 0.002$ and 0.007) (Fig. 6 c and d). Frequencies of polyfunctional CD4 T-cells did not correlate with disease outcome measures, although a weak, non-significant ($p = 0.069$), relationship was indicated six weeks following primary BCG vaccination Fig. 6e).

The functional profile of CD8 T-cell populations was primarily split between cells producing IFN-γ and TNF-α simultaneously and those producing only TNF-α (Fig. 5b). These populations were detected in all BCG vaccination groups following immunisation, although frequencies rarely reached significance above pre-vaccination levels. A significant increase in the frequency of polyfunctional CD8 T-cells was detected four weeks following *M.tb* challenge in the unvaccinated control animals ($p = 0.004$), and was accompanied by elevated frequencies of IFN-γ and TNF-α producing populations ($p = 0.004$).

3.6.3. Memory CD4 and CD8 T-cell profiles

To establish the memory differentiation status of antigen-specific CD4 and CD8 T-cells, cytokine producing central and effector memory populations were identified in each subset as cells producing any of the cytokines IFN-γ, IL-2 or TNF-α and the activation marker CD95, followed by expression patterns of the co-stimulatory receptor CD28 and lymph node homing marker CCR7. Therefore, central to effector T-cell differentiation was determined on antigen-specific CD4 and CD8 T-cells as (TCM) $CD28^{+}CCR7^{+}$; $CD28^{+}CCR7^{-}$ transitional effector memory (TransEM); and fully differentiated (TEM) $CD28^{-}CCR7^{-}$ (Fig. 7b and d).

Antigen-specific CD4 T-cells measured following BCG vaccination and *M.tb* challenge were primarily of the TransEM phenotype, expressing CD28 but not CCR7 (Fig. 7a). IV BCG vaccination induced a sustained antigen-specific TransEM response, with frequencies of this population significantly higher than those measured in the ID BCG vaccination group at weeks six, 12 and 20 post-vaccination ($p = 0.037$, 0.025 *and* 0.025, respectively). A strong boosting response was evident in the ID + IT vaccination group one week following IT BCG delivery (study week 12), with frequencies of cytokine producing TransEM populations significantly above either ID or IV BCG vaccinated groups at this time point ($p = 0.004$ and $p = 0.004$, respectively). Anamnestic cytokine responses were detected following *M.tb* challenge in the TransEM populations of ID and ID + IT BCG vaccinated animals, whereas the median frequency of cytokine producing TransEM CD4 T-cells measured in the IV vaccination group two and four weeks (study week 23 and 25) following *M.tb* inoculation, remained statistically equivalent to frequencies measured one week prior (study week 20) to challenge ($p = 0.749$ *and* 0.873, respectively). Antigen-specific TransEM frequencies were significantly above that of the unvaccinated controls at study week 23 in all vaccination groups ($p = 0.037$ and $p = 0.025$

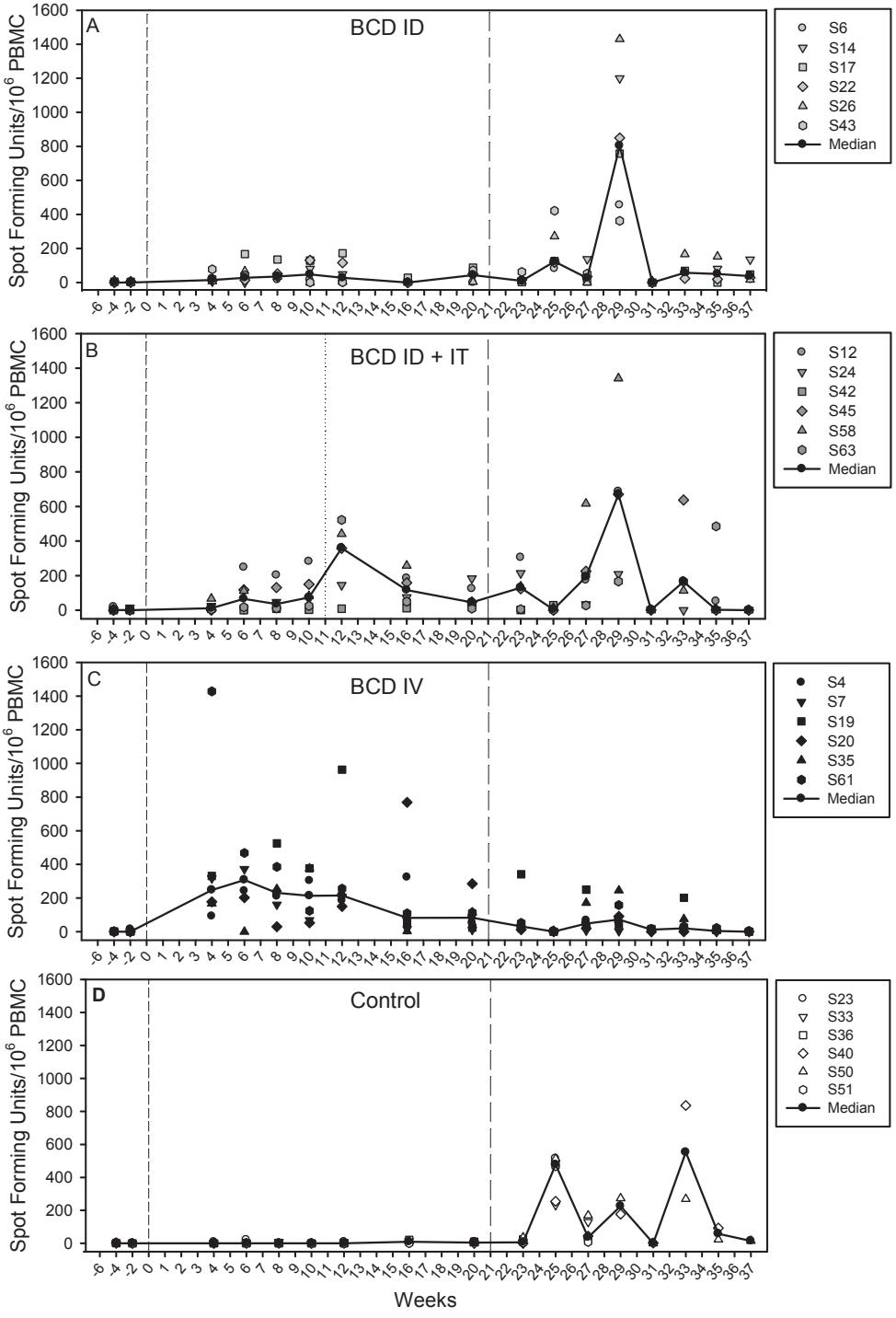

Fig. 4. Immune response to vaccination and challenge: The frequency of PPD-specific IFN-γ secreting cells measured after BCG vaccination and challenge measured by ELISpot. Panel A: response profile in Group A which received BCG as a single intradermal injection; Panel B: response profile in Group B which received BCG in a BCG ID prime/IT boost regimen; Panel C: response profile in Group C which received BCG as a single intravenous injection and Panel D shows the response in Group D which did not receive BCG vaccination. Vaccination with BCG at week 0 is indicated by the dashed line, intra-tracheal vaccination with BCG indicated by the dotted line at week 12 and aerosol exposure to *M. tuberculosis* indicated by the long dashed line at week 21.

for ID and ID + IT or IV, respectively). However, by study week 25 (four weeks post *M.tb challenge*), antigen-specific CD4 TransEM populations were statistically equivalent when compared across the treatment groups ($p > 0.05$), although there was a non-significant trend for frequencies of cytokine producing TransEM cells in the unvaccinated controls to exceed that of the BCG vaccinated animals. At this time-point, frequencies of antigen-specific TransEM cells measured in the IV vaccinated animals appeared lower than those of the other treatment groups, approaching significance in relation to the unvaccinated controls and ID vaccinated animals ($p = 0.055$ *and* 0.078, respectively). Antigen-specific CD4 TCM populations were detected in all BCG

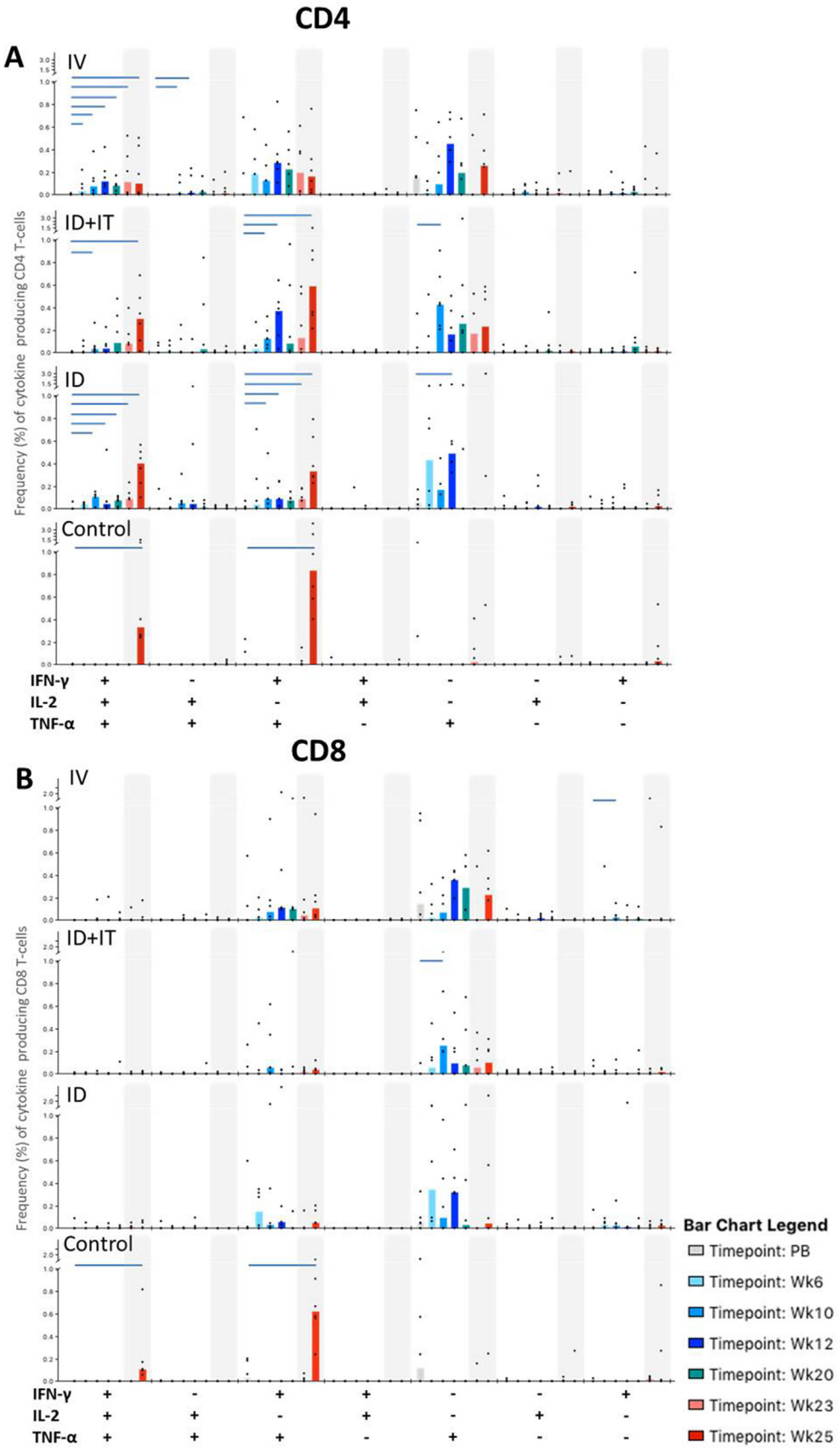

Fig. 5. PPD-specific polyfunctional CD4 and CD8 T-cell responses. Bar charts represent vaccination group median values of cytokine producing CD4 T-cells (plot A) and CD8 T cells (plot B) isolated prior to vaccination (PB) and at study weeks 6, 10, 12, 20, 23 and 25. Note that all vaccinated animals received BCG vaccinations at week 0 by intravenous (IV), or intradermal (ID and ID + IT) injection, and that the ID + IT vaccination group received a further intratracheal BCG inoculation at study week 11. Polyfunctional T-cell responses measured in unvaccinated controls are shown at PB and weeks 23 and 25. All animals received aerosol *M.tb* challenge at study week 21. Shaded areas depict immune responses measured following *M.tb* challenge. Cytokine frequencies in individual animals are represented by dots. Horizontal bars denote significant changes from mean pre-vaccination values as measured by Wilcoxon signed rank test ($p \leq 0.05$).

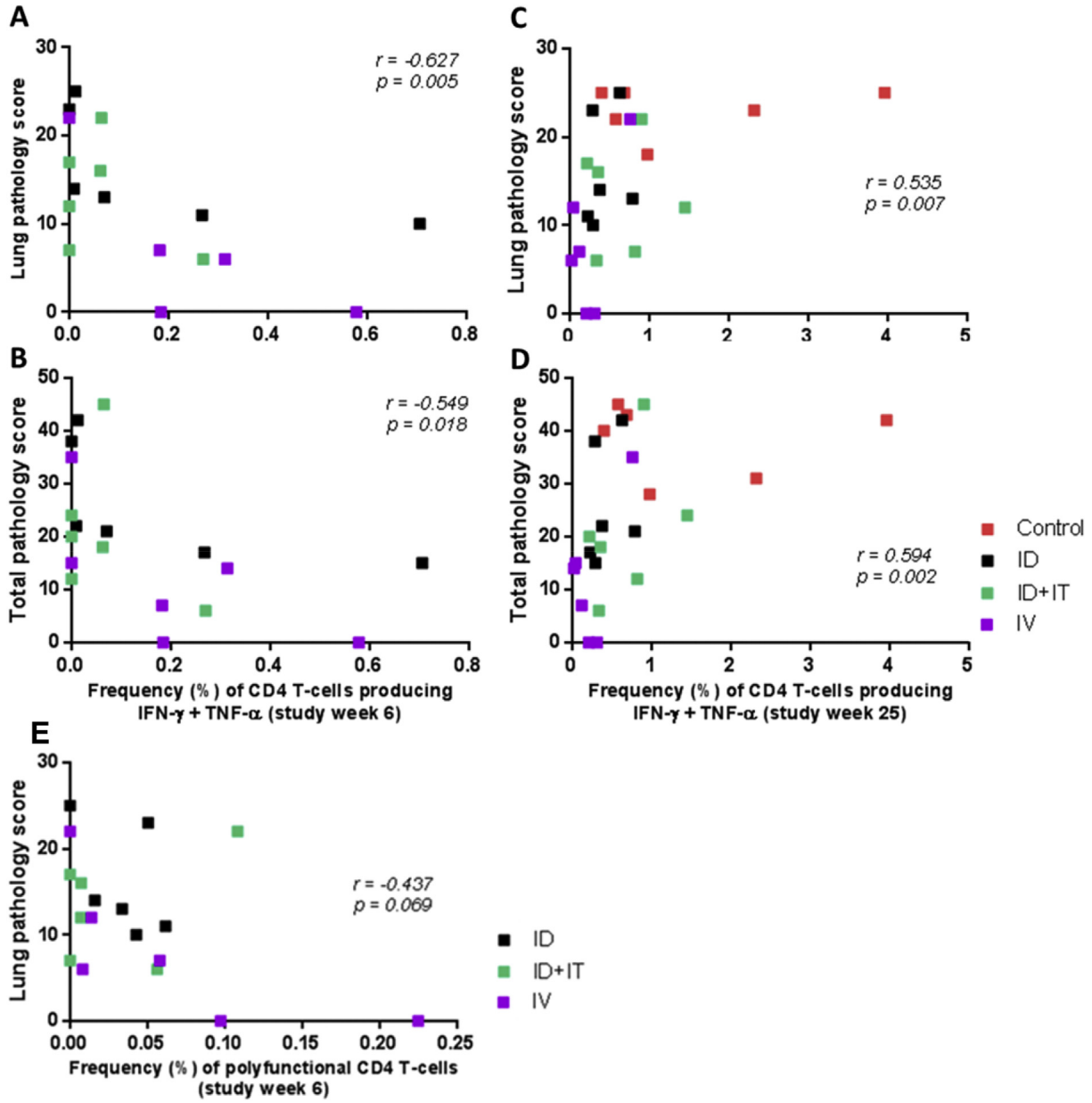

Fig. 6. Correlation plots comparing the frequency of PPD-specific CD4 T-cell populations with disease outcome measured by either lung (A, C and E) or total (B and D) pathology scores. Plots A and B show correlations between outcome and the frequency of PPD-specific CD4 T-cells producing IFN-γ and TNF-α simultaneously at six weeks following primary BCG vaccination; Plots C and D show correlations between outcome and the frequency of PPD-specific CD4 T-cells producing IFN-γ and TNF-α simultaneously four weeks following aerosol *M. tuberculosis* infection; Plot E shows a correlation plot comparing the frequency of PPD-specific polyfunctional CD4 T-cells producing IFN-γ, IL-2 and TNF-α simultaneously six weeks following primary BCG vaccination with disease outcome as measured by lung pathology score. Data points represent individual animals, and vaccination groups are indicated by colour. Spearman's correlation coefficient (r) and significance values (p) are indicated.

vaccination groups six and ten weeks after vaccination, and in ID vaccinated animals 12 weeks following vaccination, but were absent, or only detectable at low frequencies at later vaccination phase time points and following *M.tb* challenge (Fig. 7a). Frequencies of antigen-specific CD4 TEM populations were detected at low levels throughout the study and remained comparable between the treatment groups (Fig. 7a).

Cytokine production in antigen-specific CD8 memory T-cell populations was more evenly split between TransEM and TEM populations and remained relatively consistent during the period between BCG vaccination and *M.tb* challenge (Fig. 7c). No significant differences were detected between the BCG vaccination groups in terms of cytokine producing CD8 memory T-cell populations. However, the frequency of antigen-specific TransEM cells measured in the unvaccinated controls was significantly greater than that observed in the IV BCG vaccine group ($p = 0.016$), and approached significance relative to ID + IT and ID BCG vaccinated animals ($p = 0.055$ and 0.078, respectively), at study week 25.

3.6.4. Correlations between immunological assays

The *ex vivo* IFN-γ ELISpot assay applied throughout this study is commonly assumed to provide a rapid readout of Th1 effector T-cell function. To investigate the relationship between PPD-specific immune responses measured by IFN-γ ELISpot and antigen-specific

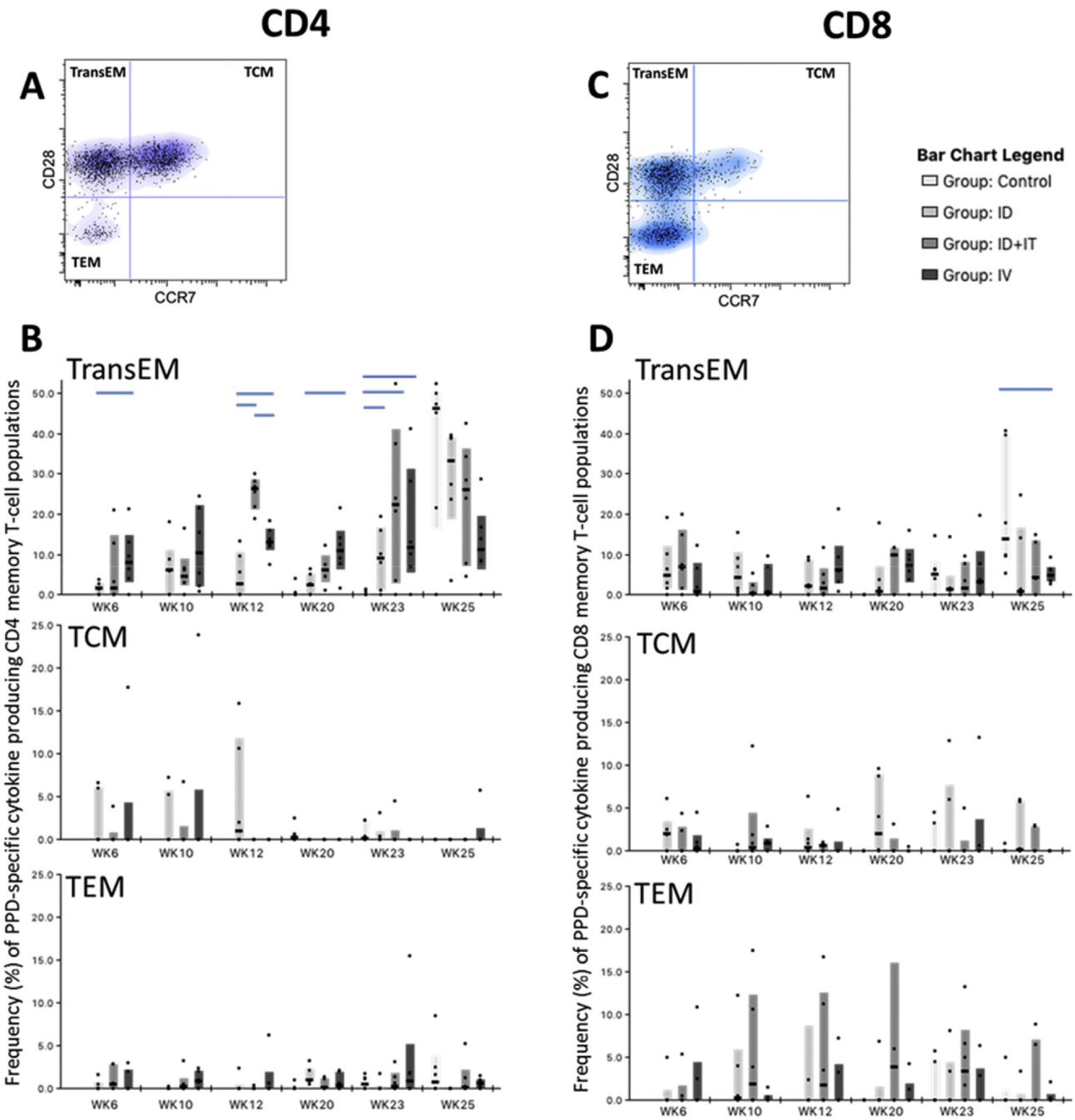

Fig. 7. Antigen-specific CD4 and CD8 memory T-cell profiles measured in PBMCs. Plots A and C, show representative bivariate density plots showing central to effector memory T-cell populations, defined by patterns of CD28 and CCR7 staining on CD95 expressing CD4 (A) and CD8 (C) T-cells, overlaid with cytokine producing cells represented as dots. Plot B displays the frequency of antigen-specific cytokine producing memory CD4 T-cell populations during the vaccination and *M.tb* infection phase of the study. Box plots show interquartile range with medians indicated. Plot C displays the frequency of antigen-specific cytokine producing memory CD8 T-cell populations during the vaccination and *M.tb* infection phase of the study. Box plots show interquartile range with medians indicated.

memory T-cell phenotype, Spearman's correlation analysis was used to compare IFN-γ SFU and antigen-specific CD4 memory T-cell frequencies measured at equivalent time-points (Fig. 8). This revealed significant correlations between IFN-γ SFU measured by ELISpot assay and antigen-specific CD4 transitional effector memory T-cell frequency at study weeks six, 12, 23 and 25 post-vaccination ($p = 0.0001$ *to* 0.02, $r = 0.515$ *to* 0.867, respectively). This indicated that *ex vivo* IFN-γ SFU measured by ELISpot assay provides a useful measure of CD4 TransEM activity.

4. Discussion

The contribution of non-human primate models in the development of new TB vaccines would be revolutionised by the identification of a vaccine strategy that can confer a clear protective effect against *M. tb* challenge. The efficacy afforded by such a strategy would enable identification of immune correlates of protection that could inform the development of new vaccines and would also provide a bench mark against which their efficacy could

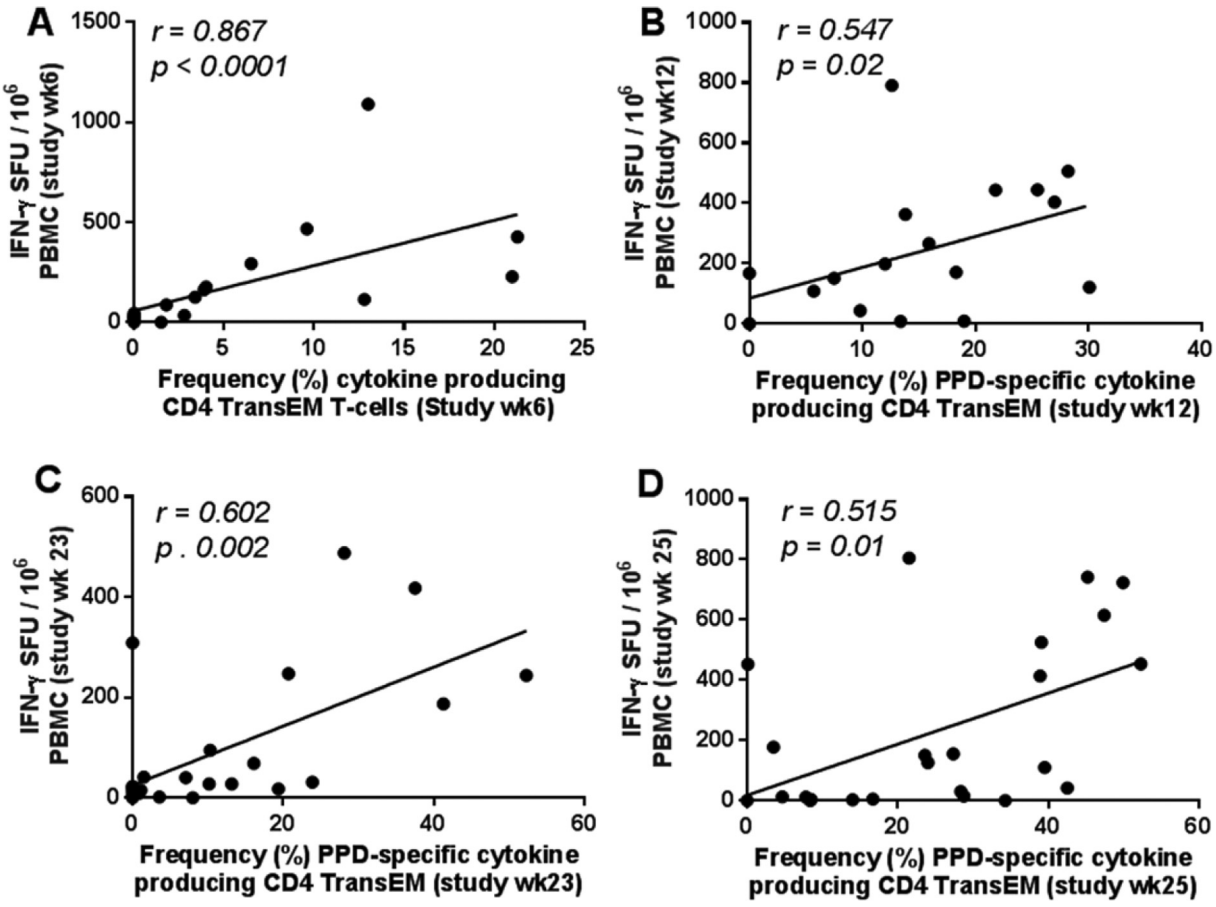

Fig. 8. Relationship between PPD-specific IFN-γ SFU measured by ELISpot and frequency of antigen-specific CD4 TransEM populations. Correlation plots comparing the PPD-specific SFU measured by ELISpot and frequency of antigen-specific CD4 Transitional effector T-cell populations at six (A), 12 (B), 23 (C) and 25 (D) weeks following primary BCG vaccination. Note that week 23 and 25 also correspond to weeks two and four following aerosol *M. tuberculosis* infection, respectively (C and D). Data points represent individual animals. Spearman's correlation coefficient (r) and significance values (p) are indicated. A linear regression line is included for reference.

be tested. This study has revealed that BCG when delivered intravenously has the potential to fulfil this role.

As the primary aim of this study was to identify vaccine strategies with enhanced protective efficacy against aerosol exposure to *M. tb*, the BCG doses used for administration were selected to increase the protective effect afforded by BCG for the specific route and not matched across delivery routes, although a limitation of this strategy precluded the dissection of the contribution of dose and route to the protective effects identified. As in previous vaccine evaluation studies in the rhesus macaque model (Sharpe 2010, Verreck 2009), and in line with the guidelines for the use of TB models of tuberculosis (Flynn, Reed & Langermans 2004), the dose recommended for intradermal immunisation of humans from an age of two years was selected for intradermal delivery to the macaques in groups A and B. The BCG dose selected for intravenous (group C) and intra-tracheal delivery (group B) were derived using a pragmatic approach. Following a review of early studies [9–12], in which large doses of older BCG strains were used, it was not possible to equate the doses quoted to exact levels of the current BCG SSI vaccine, beyond the implication that the doses used were larger than the standard human ID dose. Therefore, to mitigate risk of inducing adverse events, a dose 10 fold higher than the ID doses was selected as this has previously been shown to be well tolerated following delivery directly to the lungs (Sharpe et al., unpublished observations).

4.1. BCG dose and route influence TB-induced disease burden and dissemination

The single intradermal BCG vaccination (group A) conferred a significant improvement in the ability to control disease progression in the 17 week period after aerosol exposure and the overall disease burden measured as total gross pathology score in comparison to the outcome in unvaccinated animals. The level of efficacy measured for BCG delivered intradermally in the rhesus macaques in this study is consistent a previous study [31], which suggests that BCG can induce a consistent level of protection within this model. In addition to the improvements in disease control and overall disease burden induced by intradermal delivery of BCG alone, the application of a second vaccination, with BCG delivered directly to the lung to form a BCG ID prime/BCG IT boost regimen, led to a reduction in the level of pulmonary disease. The improved outcome afforded by BCG revaccination in this study is consistent with that seen in clinical trials [15,16] and studies in other animal models [13,14]. Although further work is required to determine the role of the delivery route and dose in the effect afforded, there have been no previous reports of BCG boosting vaccinations delivered directly to the macaque lung in a heterologous revaccination regimen, so the strong systemic immunogenicity observed in this study, and the improved outcome is a noteworthy proof of concept. Whilst intratracheal administration may not be a practical approach for mass vaccination campaigns, other mucosal

vaccination approaches such as aerosol delivery to the respiratory tract may prove a more viable strategy. Indeed an improved protective effect has been reported following delivery of BCG by aerosol, either as a primary vaccination in macaques [10] or as a booster in mice [37],

BCG delivered intravenously led to significantly improved outcomes compared to those in the unvaccinated group and the BCG ID vaccinated group, which is consistent with studies from the 1970's [9–12]; however, the study reported here provides further evidence of the robustness of the protective effect induced by IV vaccination, as a higher dose of the more virulent strain *M. tuberculosis* Erdman [38] was used for aerosol challenge. Although the intravenous route is not currently considered for use in clinical studies, this does not preclude the use of this delivery route in non-human primate studies to provide the standard against which new vaccines can be compared, or as a tool for the investigation of potential correlates of protection.

4.2. Polyfunctional T cell induction by Mycobacteria

Multifunctional T-cells are known to be a component of the response to *M. tb* infection in humans [23,39–42], and in non-human primates [31,43], and there is evidence to suggest that vaccine-induced multifunctional T-cell populations may correlate with improved outcome following virulent *M. tb* challenge [43,44]. This study confirms that polyfunctional T-cells expressing IFN-γ, IL-2 and TNF-α are induced by parenteral BCG vaccination strategies including ID and IV application. Furthermore, elevated frequencies of polyfunctional CD4 populations were also detected following high dose *M. tb* challenge, particularly in unvaccinated animals and the ID or ID + IT study groups which developed relative high levels of disease pathology in comparison to the IV vaccination group. This confirms that these T-cell populations are involved in the response during the active phase of disease [23,39–42] and indicates a possible link between polyfunctional T-cell frequency and pathogen-derived antigenic load [45]. In addition to polyfunctional cells producing IFN-γ, IL-2 and TNF-α, it was found that a major component of the BCG-induced multifunctional T-cell response was accounted for by CD4 T-cells producing IFN-γ and TNF-α in unison. Frequencies of this dual functional CD4 T-cell population remained elevated throughout the vaccination phase of the study, regardless of BCG vaccination route or regimen, and early post vaccination frequencies correlated significantly with reduced total and lung pathology score following subsequent aerosol *M. tb* challenge (Fig. 7). However, high frequencies of IFN-γ and TNF-α producing CD4 T-cells were also detected following *M. tb* challenge in unvaccinated controls and in the animals receiving less protective vaccination regimens (ID and ID + IT). Correlation analysis applied at this stage of the study revealed a significant relationship between the frequency of this T-cell population and the development of pulmonary and disseminated disease pathology (Fig. 7). These correlative analyses indicate that CD4 T-cells producing IFN-γ and TNF-α simultaneously are a key effector population in the mycobacteria-specific T-cell response, including during the early stages of *M. tb* infection, and is in agreement with observations reported from functional T-cell studies conducted using samples from active TB patients [46].

In contrast to the functional repertoire observed in CD4 T-cells, significant increases in the frequency of multifunctional CD8 subsets were only detected in unvaccinated control animals, four weeks following *M. tb* exposure. However, as low levels of IFN-γ and TNF-α secreting CD8 population were detected in the IV BCG vaccinated animals, which persisted until time-points immediately prior to *M. tb* challenge, these cells may have contributed to the strong protective efficacy observed in this group.

4.3. Protection associated with mycobacterial antigen-specific CD4 effector memory T-cell populations

Intradermal BCG vaccination is known to protect infants and children against severe disseminated forms of TB [47,48]. However, this protective immunity is less evident in the adult population for whom the efficacy of BCG vaccination is highly variable [4,49]. Conventionally, the phenotypic composition of the vaccine-induced memory T-cell population is considered indicative of the long-term persistence of the vaccine mediated response, with TCM populations key to long term immunity [50,51]. It has been suggested that a poor capacity to induce TCM populations is an underlying factor in the failure of BCG to protect beyond adolescence in the human population [29], and the BCG mediated memory T-cell response has been shown to favour induction of effector T-cell populations [28,52]. The antigen-specific memory T-cell analysis applied during this study provides further evidence that memory T-cell populations induced by BCG vaccination are biased toward an effector phenotype, with the CD4 transitional effector memory T-cell population found to dominate the antigen-specific vaccine induced response, as well as the response to *M. tb* infection. This finding is in close agreement with memory T-cell frequencies observed in human TB infection where an analogous effector T-cell population, expressing the same profile of cytokines, has been shown to predominate in peripheral blood samples collected from active TB patients [46]. In our study, IV BCG inoculation induced a sustained expansion of this systemic mycobacterial antigen-specific CD4 effector memory population, which remained significantly elevated above that observed in ID BCG vaccinated animals one week prior to *M. tb* challenge ($P = 0.025$). Heightened mycobacteria-specific CD4 TEM responses prior to infection may represent a potential biomarker of protection against high dose *M. tb* challenge.

IFN-γ ELISpot profiles and the antigen-specific memory T-cell response identified the lack of a systemic, anamnestic response post-*M. tb* challenge in the highly protected IV BCG vaccination group. It is possible that immunological control was enacted at the primary site of infection through heightened levels of CD4 effector T-cell activity within the lung and associated lymphoid tissues, although increased activation and activity from the innate components of the cellular immune response may also have contributed to this control. This observation is analogous to the recent findings reported from rhesus macaque studies investigating the efficacy of cytomegalovirus (CMV) vectored vaccine constructs against experimental simian immunodeficiency virus (SIV) infection [53]. These vaccine constructs were designed to persist within the host organism as a strategy to maintain elevated frequencies of SIV-specific effector T-cell populations, and have been shown capable of imparting significant and long term protection against high dose mucosal SIV challenge. Interestingly, whilst increased post-vaccination frequencies of SIV-specific effector memory T-cell populations were shown to correspond to the likely subsequent control of SIV infection, animals which controlled disease made no post-SIV challenge anamnestic response, thus indicating that vaccine induced effector T-cell populations were able to control the infectious challenge within the mucosal tissues during the early stages of infection [53,54]. As innate mechanisms were unlikely to be responsible for protection against SIV infection [55,56], these studies strongly support the premise that effector T-cell populations were responsible for the protection imparted by these vaccination regimens, although the mechanism remains to be elucidated [53,54]. Nevertheless, as the BCG-induced T-cell response clearly supported the induction of CD4 effector memory T-cell responses, there is a clear parallel between the immunological parameters and protection observed in our study and those

observed following vaccination with the protective CMV/SIV effector T-cell targeted vaccination strategy. Further studies conducted over extended timescales are required to assess the likely persistence of this protection, and to establish whether high frequencies of IV BCG-induced mycobacteria-specific effector T-cell populations are able to impart long term protection against *M. tb* infection and disease.

5. Conclusion

This study has shown that BCG vaccination was able to significantly reduce disease severity induced by high dose aerosol *M. tb* challenge in the rhesus macaque model, and that this protection can be improved by mucosal BCG revaccination regimens or by systemic BCG vaccination delivered intravenously. Whilst it is recognised that neither IV nor IT BCG delivery strategies are appropriate for deployment in the clinical setting, recent NHP vaccine evaluation studies and early stage clinical trials have demonstrated that alternative vaccination strategies such as aerosol delivery are a practical, safe and immunogenic approach for the delivery of TB vaccines [43,44,57–60]. The identification of IV-delivered BCG as a highly protective vaccination strategy may prove a pivotal step towards deciphering protective immunological mechanisms against *M. tb* infection in pre-clinical models, potentially leading to the identification of immune correlates of protection, which could be used to accelerate the vaccine development pipeline.

Acknowledgements

This work was supported by the Department of Health, UK (Grant number 104368). The views expressed in this publication are those of the authors and not necessarily those of the Department of Health. We thank the staff of the Biological Investigations Group at PHE Porton and the PHE macaque colonies for assistance in conducting studies, Charlotte Hall and Dominic Kelly for bacteriology and aerobiology support, and Kim Hatch and Laura Hunter for histology support.

References

[1] WHO. WHO, Global tuberculosis report, 2014. WHO; 2014. http://www.who.int/tb/publications/global_report/en/ (accessed October 27, 2015).
[2] Zumla A, George A, Sharma V, Herbert RHN. Baroness Masham of Ilton, A. Oxley, M. Oliver, the WHO 2014 global tuberculosis report–further to go. Lancet Glob Health 2015;3:e10–12. http://dx.doi.org/10.1016/S2214-109X(14)70361-4.
[3] Trunz BB, Fine P, Dye C. Effect of BCG vaccination on childhood tuberculous meningitis and miliary tuberculosis worldwide: a meta-analysis and assessment of cost-effectiveness. Lancet 2006;367:1173–80. http://dx.doi.org/10.1016/S0140-6736(06)68507-3.
[4] Colditz GA, Brewer TF, Berkey CS, Burdick E, Fineberg HV, Mosteller F. Efficacy of BCG vaccine in the prevention of tuberculosis. Meta-analysis of the published literature. JAMA 1994;271:698–702.
[5] Tameris MD, Hatherill M, Landry BS, Scriba TJ, Snowden MA, Lockhart S, et al. Safety and efficacy of MVA85A, a new tuberculosis vaccine, in infants previously vaccinated with BCG: a randomised, placebo-controlled phase 2b trial. Lancet 2013;381:1021–8. http://dx.doi.org/10.1016/S0140-6736(13)60177-4.
[6] Kaushal D, Mehra S, Didier PJ, Lackner AA. The non-human primate model of tuberculosis. J Med Primatol 2012;41:191–201. http://dx.doi.org/10.1111/j.1600-0684.2012.00536.x.
[7] Peña JC, Ho W-Z. Monkey models of tuberculosis: lessons learned. Infect Immun 2015;83:852–62. http://dx.doi.org/10.1128/IAI.02850-14.
[8] Scanga CA, Flynn JL. Modeling tuberculosis in nonhuman primates. Cold Spring Harb Perspect Med 2014;4:a018564. http://dx.doi.org/10.1101/cshperspect.a018564.
[9] Anacker RL, Brehmer W, Barclay WR, Leif WR, Ribi E, Simmons JH, et al. Superiority of intravenously administered BCG and BCG cell walls in protecting rhesus monkeys (Macaca mulatta) against airborne tuberculosis. Z. Für Immun. Exp Klin Immunol 1972;143:363–76.
[10] Barclay WR, Busey WM, Dalgard DW, Good RC, Janicki BW, Kasik JE, et al. Protection of monkeys against airborne tuberculosis by aerosol vaccination with bacillus Calmette-Guerin. Am Rev Respir Dis 1973;107:351–8.
[11] Barclay WR, Anacker RL, Brehmer W, Leif W, Ribi E. Aerosol-induced tuberculosis in subhuman primates and the course of the disease after intravenous BCG vaccination. Infect Immun 1970;2:574–82.
[12] Ribi E, Anacker RL, Barclay WR, Brehmer W, Harris SC, Leif WR, et al. Efficacy of mycobacterial cell walls as a vaccine against airborne tuberculosis in the rhesus monkey. J Infect Dis 1971;123:527–38.
[13] Parlane NA, Shu D, Subharat S, Wedlock DN, Rehm BHA, de Lisle GW, et al. Revaccination of cattle with bacille Calmette-Guérin two years after first vaccination when immunity has waned, boosted protection against challenge with Mycobacterium bovis. PloS One 2014;9:e106519. http://dx.doi.org/10.1371/journal.pone.0106519.
[14] Li W, Huang H, Hua W, Ben S, Liu H, Xu B, et al. Neonatal revaccination with Bacillus Calmette-Guérin elicits improved, early protection against Mycobacterium tuberculosis in mice. Vaccine 2012;30:3223–30. http://dx.doi.org/10.1016/j.vaccine.2012.02.014.
[15] Barreto ML, Pereira SM, Pilger D, Cruz AA, Cunha SS, Sant'Anna C, et al. Evidence of an effect of BCG revaccination on incidence of tuberculosis in school-aged children in Brazil: second report of the BCG-REVAC cluster-randomised trial. Vaccine 2011;29:4875–7. http://dx.doi.org/10.1016/j.vaccine.2011.05.023.
[16] Leung CC, Tam CM, Chan SL, Chan-Yeung M, Chan CK, Chang KC. Efficacy of the BCG revaccination programme in a cohort given BCG vaccination at birth in Hong Kong. Int J Tuberc Lung Dis Off J Int Union Tuberc Lung Dis 2001;5:717–23.
[17] Aguilo N, Toledo AM, Lopez-Roman EM, Perez-Herran E, Gormley E, Rullas-Trincado J, et al. Pulmonary Mycobacterium bovis BCG vaccination confers dose-dependent superior protection compared to that of subcutaneous vaccination. Clin Vaccine Immunol CVI 2014;21:594–7. http://dx.doi.org/10.1128/CVI.00700-13.
[18] Goonetilleke NP, McShane H, Hannan CM, Anderson RJ, Brookes RH, Hill AVS, et al. Against Mycobacterium tuberculosis of bacille calmette-guérin vaccine using mucosal administration and boosting with a recombinant modified vaccinia virus ankara. J Immunol 2003;171:1602–9. http://dx.doi.org/10.4049/jimmunol.171.3.1602.
[19] Haile M, Hamasur B, Jaxmar T, Gavier-Widen D, Chambers MA, Sanchez B, et al. Nasal boost with adjuvanted heat-killed BCG or arabinomannan-protein conjugate improves primary BCG-induced protection in C57BL/6 mice. Tuberc Edinb Scotl 2005;85:107–14. http://dx.doi.org/10.1016/j.tube.2004.09.013.
[20] Chackerian AA, Perera TV, Behar SM. Gamma interferon-producing CD4+ T lymphocytes in the lung correlate with resistance to infection with Mycobacterium tuberculosis. Infect Immun 2001;69:2666–74. http://dx.doi.org/10.1128/IAI.69.4.2666-2674.2001.
[21] Chen CY, Huang D, Wang RC, Shen L, Zeng G, Yao S, et al. A critical role for CD8 T cells in a nonhuman primate model of tuberculosis. PLoS Pathog 2009;5:e1000392. http://dx.doi.org/10.1371/journal.ppat.1000392.
[22] Seder RA, Darrah PA, Roederer M. T-cell quality in memory and protection: implications for vaccine design. Nat Rev Immunol 2008;8:247–58. http://dx.doi.org/10.1038/nri2274.
[23] Caccamo N, Guggino G, Joosten SA, Gelsomino G, Di Carlo P, Titone L, et al. Multifunctional CD4(+) T cells correlate with active Mycobacterium tuberculosis infection. Eur J Immunol 2010;40:2211–20. http://dx.doi.org/10.1002/eji.201040455.
[24] Darrah PA, Patel DT, De Luca PM, Lindsay RWB, Davey DF, Flynn BJ, et al. Multifunctional TH1 cells define a correlate of vaccine-mediated protection against Leishmania major. Nat Med 2007;13:843–50. http://dx.doi.org/10.1038/nm1592.
[25] Lindenstrøm T, Agger EM, Korsholm KS, Darrah PA, Aagaard C, Seder RA, et al. Tuberculosis subunit vaccination provides long-term protective immunity characterized by multifunctional CD4 memory T cells. J Immunol Balt Md 2009;1950(182):8047–55. http://dx.doi.org/10.4049/jimmunol.0801592.
[26] Aagaard C, Hoang TTKT, Izzo A, Billeskov R, Troudt J, Arnett K, et al. Cells induced by Ag85B-TB10.4/IC31® against Mycobacterium tuberculosis is highly dependent on the antigen dose. PLoS One 2009;4:e5930. http://dx.doi.org/10.1371/journal.pone.0005930.
[27] Kagina BMN, Abel B, Scriba TJ, Hughes EJ, Keyser A, Soares A, et al., other members of the South African Tuberculosis Vaccine Initiative. Specific T cell frequency and cytokine expression profile do not correlate with protection against tuberculosis after bacillus Calmette-Guérin vaccination of newborns. Am J Respir Crit Care Med 2010;182:1073–9. http://dx.doi.org/10.1164/rccm.201003-0334OC.
[28] Kaveh DA, Bachy VS, Hewinson RG, Hogarth PJ. Systemic BCG immunization induces persistent lung mucosal multifunctional CD4 TEM cells which expand following virulent mycobacterial challenge. PLoS One 2011;6:e21566. http://dx.doi.org/10.1371/journal.pone.0021566.
[29] Orme IM. The achilles heel of BCG. Tuberc. Edinb Scotl 2010;90:329–32. http://dx.doi.org/10.1016/j.tube.2010.06.002.
[30] Clark SO, Hall Y, Kelly DLF, Hatch GJ, Williams A. Survival of Mycobacterium tuberculosis during experimental aerosolization and implications for aerosol challenge models. J Appl Microbiol 2011;111:350–9. http://dx.doi.org/10.1111/j.1365-2672.2011.05069.x.
[31] Sharpe SA, McShane H, Dennis MJ, Basaraba RJ, Gleeson F, Hall G, et al. Establishment of an aerosol challenge model of tuberculosis in rhesus macaques and an evaluation of endpoints for vaccine testing. Clin Vaccine Immunol CVI 2010;17:1170–82. http://dx.doi.org/10.1128/CVI.00079-10.
[32] Sharpe SA, Eschelbach E, Basaraba RJ, Gleeson F, Hall GA, McIntyre A, et al.

Determination of lesion volume by MRI and stereology in a macaque model of tuberculosis. Tuberculosis 2009;89:405–16. http://dx.doi.org/10.1016/j.tube.2009.09.002.
[33] Druett HA. A mobile form of the Henderson apparatus. J Hyg (Lond) 1969;67:437–48.
[34] Harper GJ, Morton JD. The respiratory retention of bacterial aerosols: experiments with radioactive spores. Epidemiol. Infect 1953;51:372–85. http://dx.doi.org/10.1017/S0022172400015801.
[35] Rayner EL, Pearson GR, Hall GA, Gleeson F, McIntyre A, Smyth D, et al. Early lesions following aerosol challenge of rhesus macaques (Macaca mulatta) with Mycobacterium tuberculosis (Erdman strain). J Comp Pathol 2015;152:217–26. http://dx.doi.org/10.1016/j.jcpa.2014.10.002.
[36] Roederer M, Nozzi JL, Nason MC. SPICE: exploration and analysis of post-cytometric complex multivariate datasets. Cytom Part J Int Soc Anal Cytol 2011;79:167–74. http://dx.doi.org/10.1002/cyto.a.21015.
[37] Cha SB, Kim WS, Kim J-S, Kim H, Kwon KW, Han SJ, et al. Repeated aerosolized-boosting with gamma-irradiated mycobacterium bovis BCG confers improved pulmonary protection against the hypervirulent Mycobacterium tuberculosis strain HN878 in mice. PLoS One 2015;10. http://dx.doi.org/10.1371/journal.pone.0141577.
[38] Gormus BJ, Blanchard JL, Alvarez XH, Didier PJ. Evidence for a rhesus monkey model of asymptomatic tuberculosis. J Med Primatol 2004;33:134–45. http://dx.doi.org/10.1111/j.1600-0684.2004.00062.x.
[39] Mueller H, Detjen AK, Schuck SD, Gutschmidt A, Wahn U, Magdorf K, et al. Mycobacterium tuberculosis-specific CD4+, IFNγ+, and TNFα+ multifunctional memory T cells coexpress GM-CSF. Cytokine 2008;43:143–8. http://dx.doi.org/10.1016/j.cyto.2008.05.002.
[40] Qiu Z, Zhang M, Zhu Y, Zheng F, Lu P, Liu H, et al. Multifunctional CD4 T cell responses in patients with active tuberculosis. Sci Rep 2012;2. http://dx.doi.org/10.1038/srep00216.
[41] Sutherland JS, Adetifa IM, Hill PC, Adegbola RA, Ota MOC. Pattern and diversity of cytokine production differentiates between Mycobacterium tuberculosis infection and disease. Eur J Immunol 2009;39:723–9. http://dx.doi.org/10.1002/eji.200838693.
[42] Young JM, Adetifa IMO, Ota MOC, Sutherland JS. Expanded polyfunctional T cell response to mycobacterial antigens in TB disease and contraction post-treatment. PLoS One 2010;5:e11237. http://dx.doi.org/10.1371/journal.pone.0011237.
[43] Darrah PA, Bolton DL, Lackner AA, Kaushal D, Aye PP, Mehra S, et al. Aerosol vaccination with AERAS-402 elicits robust cellular immune responses in the lungs of rhesus macaques but fails to protect against high-dose Mycobacterium tuberculosis challenge. J Immunol Balt Md 1950 2014;193:1799–811. http://dx.doi.org/10.4049/jimmunol.1400676.
[44] Kaushal D, Foreman TW, Gautam US, Alvarez X, Adekambi T, Rangel-Moreno J, et al. Mucosal vaccination with attenuated Mycobacterium tuberculosis induces strong central memory responses and protects against tuberculosis. Nat Commun 2015;6:8533. http://dx.doi.org/10.1038/ncomms9533.
[45] Day CL, Abrahams DA, Lerumo L, van Rensburg EJ, Stone L, O'rie T, et al. Functional capacity of Mycobacterium tuberculosis-specific T cell responses in humans is associated with mycobacterial load. J Immunol Balt Md 1950 2011;187:2222–32. http://dx.doi.org/10.4049/jimmunol.1101122.
[46] Petruccioli E, Petrone L, Vanini V, Sampaolesi A, Gualano G, Girardi E, et al. IFNγ/TNFα specific-cells and effector memory phenotype associate with active tuberculosis. J Infect 2013;66:475–86. http://dx.doi.org/10.1016/j.jinf.2013.02.004.
[47] Mangtani P, Abubakar I, Ariti C, Beynon R, Pimpin L, Fine PEM, et al. Protection by BCG vaccine against tuberculosis: a systematic review of randomized controlled trials. Clin Infect Dis Off Publ Infect Dis Soc Am 2014;58:470–80. http://dx.doi.org/10.1093/cid/cit790.
[48] Roy A, Eisenhut M, Harris RJ, Rodrigues LC, Sridhar S, Habermann S, et al. Effect of BCG vaccination against Mycobacterium tuberculosis infection in children: systematic review and meta-analysis. BMJ 2014;349. g4643.
[49] Sterne JA, Rodrigues LC, Guedes IN. Does the efficacy of BCG decline with time since vaccination? Int J Tuberc Lung Dis Off J Int Union Tuberc Lung Dis 1998;2:200–7.
[50] Lanzavecchia A, Sallusto F. Understanding the generation and function of memory T cell subsets. Curr Opin Immunol 2005;17:326–32. http://dx.doi.org/10.1016/j.coi.2005.04.010.
[51] Sallusto F, Lenig D, Förster R, Lipp M, Lanzavecchia A. Two subsets of memory T lymphocytes with distinct homing potentials and effector functions. Nature 1999;401:708–12. http://dx.doi.org/10.1038/44385.
[52] Henao-Tamayo MI, Ordway DJ, Irwin SM, Shang S, Shanley C, Orme IM. Phenotypic definition of effector and memory T-lymphocyte subsets in mice chronically infected with mycobacterium tuberculosis. Clin Vaccine Immunol 2010;17:618–25. http://dx.doi.org/10.1128/CVI.00368-09.
[53] Hansen SG, Ford JC, Lewis MS, Ventura AB, Hughes CM, Coyne-Johnson L, et al. Profound early control of highly pathogenic SIV by an effector-memory T cell vaccine. Nature 2011;473:523–7. http://dx.doi.org/10.1038/nature10003.
[54] Masopust D, Picker LJ. Hidden memories: front line memory T cells and early pathogen interception. J Immunol Balt Md 2012;1950(188):5811–7. http://dx.doi.org/10.4049/jimmunol.1102695.
[55] Haase AT. Early events in sexual transmission of HIV and SIV and opportunities for interventions. Annu Rev Med 2011;62:127–39. http://dx.doi.org/10.1146/annurev-med-080709-124959.
[56] Wang Y, Abel K, Lantz K, Krieg AM, McChesney MB, Miller CJ. The toll-like receptor 7 (TLR7) agonist, imiquimod, and the TLR9 agonist, CpG ODN, induce antiviral cytokines and chemokines but do not prevent vaginal transmission of simian immunodeficiency virus when applied intravaginally to rhesus macaques. J Virol 2005;79:14355–70. http://dx.doi.org/10.1128/JVI.79.22.14355-14370.2005.
[57] Jeyanathan M, Thanthrige-Don N, Afkhami S, Lai R, Damjanovic D, Zganiacz A, et al. Novel chimpanzee adenovirus-vectored respiratory mucosal tuberculosis vaccine: overcoming local anti-human adenovirus immunity for potent TB protection. Mucosal Immunol 2015;8:1373–87. http://dx.doi.org/10.1038/mi.2015.29.
[58] Satti I, Meyer J, Harris SA, Thomas Z-RM, Griffiths K, Antrobus RD, et al. Safety and immunogenicity of a candidate tuberculosis vaccine MVA85A delivered by aerosol in BCG-vaccinated healthy adults: a phase 1, double-blind, randomised controlled trial. Lancet Infect Dis 2014;14:939–46. http://dx.doi.org/10.1016/S1473-3099(14)70845-X.
[59] White AD, Sarfas C, West K, Sibley LS, Wareham AS, Clark S, et al. An evaluation of the immunogenicity of BCG, delivered by aerosol to the lungs of macaques. Clin Vaccine Immunol CVI 2015. http://dx.doi.org/10.1128/CVI.00289-15.
[60] White AD, Sibley L, Dennis MJ, Gooch K, Betts G, Edwards N, et al. Evaluation of the safety and immunogenicity of a candidate tuberculosis vaccine, MVA85A, delivered by aerosol to the lungs of macaques. Clin Vaccine Immunol CVI 2013;20:663–72. http://dx.doi.org/10.1128/CVI.00690-12.